0 NOV. 1970

ICAS Paper No. 70–15

LIFTING AEROFOILS WITH SUPERCRITICAL SHOCKLESS FLOW

by
J. W. Boerstoel and
R. Uijlenhoet, Engineers
National Aerospace Laboratory (NLR)
Aerodynamics Division
Amsterdam, The Netherlands

The Seventh Congress of the International Council of the Aeronautical Sciences

CONSIGLIO NAZIONALE DELLE RICERCHE, ROMA, ITALY / SEPTEMBER 14-18, 1970

Price: 400 Lire

LIFTING AEROFOILS WITH SUPERCRITICAL SHOCK-FREE FLOW

J.W. Boerstoel and R. Uijlenhoet

National Aerospace Laboratory NLR, Amsterdam,

the Netherlands

Abstract

Nieuwlands hodograph theory for lifting quasi-elliptioal aerofoils has been applied to compute a number of profiles with supercritical shook-free flow at the design condition. These profiles appear to have nose camber only. The pressure distribution at the design condition is of the peaky type. The minimum radius of curvature at the nose is of the order of 0.2 % to 1½ % of the chord length. It is possible to compute the co-ordinates with sufficient precision for engineering applications.

The shapes of the profiles computed depend upon seven parameters. It appears, that four of these parameters have to be chosen carefully in order to avoid limit lines or branch points in that part of the physical plane, which is of interest.

One of the profiles has been tested in the NLR Pilot tunnel to investigate : a the effect of viscosity on the theoretical results; b the off-design behaviour. The pressure distribution in the experimental design condition (this is the condition with the weakest shocks) indicates practically shock-free flow. A 20 % loss in lift is found at this condition. By deflecting a trailing-edge flap the lift loss oould be reduced to 10 % without worsening the drag characteristics. The margin between rapid drag rise boundary and buffet boundary at high Mach numbers appeared to be small.

Notations

c_d	drag coefficient
c_ℓ	lift coefficient
c_p	pressure coefficient
M^c	local Mach number at profile tail
M_{loc}	local Mach number
M_∞	free-stream Mach number
p/p_o	ratio of local static pressure to total pressure
Re	Reynolds number based on model chord
t/c	thickness ratio of profile
x/c	chordwise co-ordinate normalised by chord length
y/c	oo-ordinate normal to chord normalised by chord length
α	incidence of ellipse in incompressible flow, or : model incidence
Γ	circulation of flow
δ	trailing-edge flap deflection angle
ε_o	parameter determining thickness ratio $\frac{1-\varepsilon_o}{1+\varepsilon_o}$ of ellipse in incompressible flow
θ_c	flow angle at tail of profile
μ	parameter determining profile slope in stagnation point on the nose

1 Introduction

Theoretical design of aerofoil sections with supercritical shock-free flow is possible using either analytical or numerical hodograph methods for potential flows, or finite difference methods applied to the non-linear Euler equations for flows which may be rotational. The analytical hodograph approach has been applied by Nieuwland to develop a theory for quasi-elliptical profiles (1). Nieuwland's theory was first used to compute the flow around a number of symmetrioal non-lifting profiles (2,3). Wind tunnel tests were performed on some of these profiles (4,5,6).

During the last two years results of the computation of lifting profiles have become available. About twenty-five profiles having supercritical flow at the design conditions have been computed. Because the theoretical pressure distribution of a profile can only be computed at the design condition of that profile, it was necessary to set up wind tunnel experiments in order to determine the off-design behaviour of the profiles. Moreover, because Nieuwland's hodograph theory is a potential theory, the computationsdo not take into account viscosity. Hence, wind tunnel tests were also used to assess the effects of viscosity on the flow.

The purpose of this paper is to present the main theoretical and experimental results obtained at NLR in the last two years.

2 Results of hodograph theory

Nieuwland's theory is a method for the transformation of the incompressible potential flow around a lifting ellipse into a compressible potential flow around a lifting quasi-elliptical profile (fig.1). In this theory four parameters appear, namely the incidence α of the ellipse in the incompressible flow, a term ε_o in the expression $\frac{1-\varepsilon_o}{1+\varepsilon_o}$ for the thickness ratio of the ellipse, the circulation Γ of the flow, and the free-stream Mach number M_∞. These four parameters define a transformation of incompressible flows around ellipses into a class of compressible flows. This transformation has been schematically represented in the first part of fig.1.

It was found that these four-parameter profiles are not closed at the rear end. A special correction function was developed in order to make the profiles closed. This correction function depends also on four parameters. These are the free-stream Mach number M_∞, the local Mach number M_c and the local flow angle θ_c at the tail of the closed profile (as the tails appeared to be cusped, it makes sense

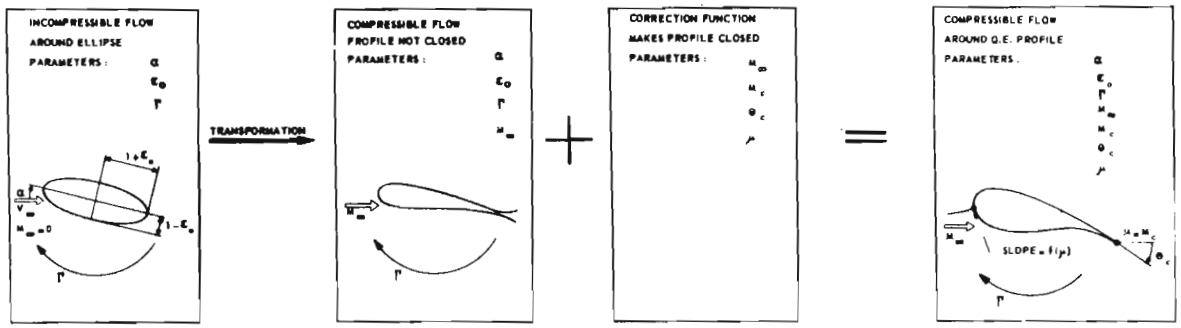

FIG. 1 SCHEME OF QUASI-ELLIPTICAL PROFILE THEORY.

to speak of the flow angle at the tail), and a parameter determining the profile slope at the nose stagnation point. The correction function was combined with the four-parameter class of compressible flows so as to give a seven parameter class of compressible flows around closed quasi-elliptical profiles. This has been schematically represented in fig.1.

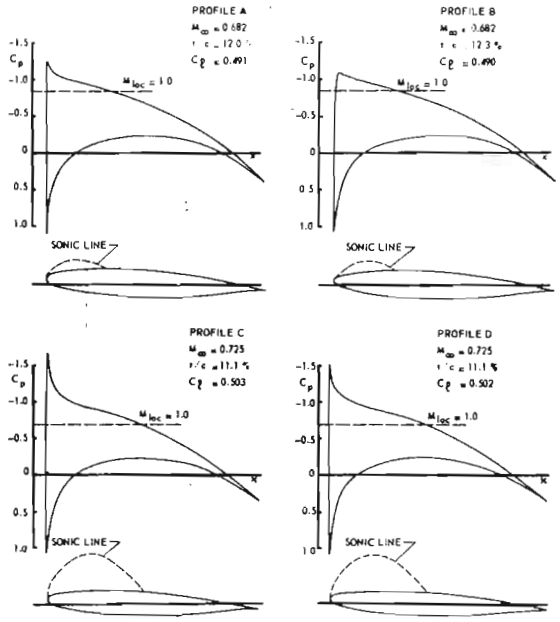

FIG. 2 SHAPE AND PRESSURE DISTRIBUTION IN THE DESIGN CONDITION OF SOME TYPICAL QUASI-ELLIPTICAL PROFILES.

Typical results of the computation of a number of seven-parameter profiles are given in fig.2 (7). The lift coefficient is 0,5. Two profiles have a thickness ratio of 12 % and a free-stream Mach number M_∞ = .682, two other profiles have a thickness ratio of 11 % and a free-stream Mach number M_∞ = .725. The pressure distributions in the design condition are of the peaky type. The height of the supersonic region is of the order of the profile thickness.

The noses of the profiles have been plotted in fig.3. The minimum radius of curvature is small, namely between 0.2 and 1.6% of the chord. The profiles are almost symmetrical with a slight amount of nose camber.

It is possible to compute profiles at other free-stream Mach numbers, other lift coefficients and other thickness ratio's by varying M_∞, Γ and ε_o respectively. It appears that the remaining parameters α, M_c, θ_c and μ can be varied only in a small range of admissable values once M_∞, Γ and ε_o have been chosen. A typical example of the determination of a range of admissable values for M_c and θ_c for a given combination of the other parameters, where μ was determined so that the correction function was as small as possible in a certain sense (for details see (1)) is given in fig.4. Outside the admissable range the regularity of the flow is destroyed by limit lines or branch points.

It has been found that the four parameters α, M_c, θ_c and μ have a large effect upon the nose shape and thus on the pressure distribution on the nose. This is illustrated in fig.3; profile A and B differ only in M_c : profile A has M_c = .5232 and profile B has M_c = .5253.

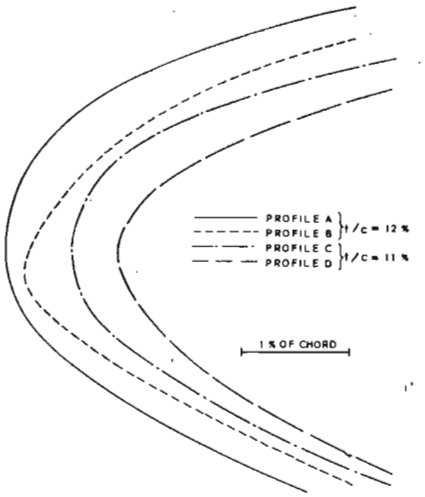

FIG. 3 TYPICAL QUASI - ELLIPTICAL PROFILE NOSES.

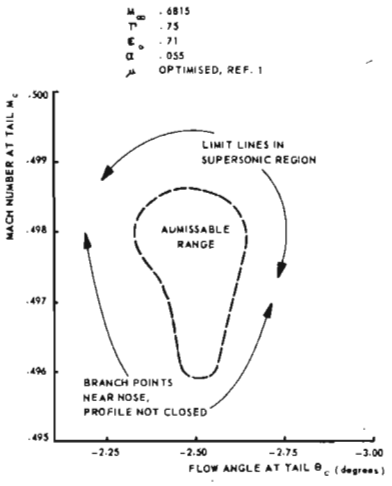

FIG. 4 EXAMPLE OF ADMISSABLE RANGE FOR M_c AND θ_c

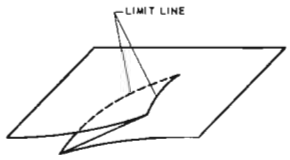

FIG. 5 FOLD OF PHYSICAL PLANE DUE TO LIMIT LINE.

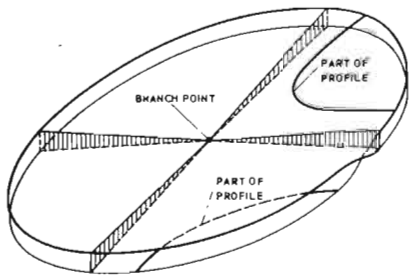

FIG. 6 PHYSICAL PLANE WITH TWO SHEETS GENERATED BY A BRANCH POINT.

The fact that limit lines may destroy the regularity of the physical plane in the supersonic region is well known. In that case the physical plane has a fold like illustrated in fig.5.

The regularity of the physical plane may also be destroyed by branch points. The physical plane consists then of at least two sheets like illustrated in fig.6. It has been found, that the quasi-elliptical profiles have a branch point in the low-speed region near the nose. If the branch point is situated inside the profile this is acceptable; if not it is not possible to make the profile closed at the nose, for the image of the profile then lies in different sheets (fig.6). Another property which makes it impossible to obtain a physically meaningful interpretation in this situation is that in the branch point two streamlines form a cusp.

The profiles can be computed sufficiently accurately for engineering applications in aeronautics. In a complete computation of a profile the ordinates, slope and radius of curvature are determined in about 200 points together with the pressure coefficients. The precision of these data is equal to or better than the following values :

co-ordinates	.002 % of the chord
slopes	.05 degrees
radii of curvature	.1 % of the local radius of curvature
pressure coefficients c_p	.001

The profile used in the experiments was computed to this accuracy.

The seven parameters of the profile E[8] that was tested were determined by first maximizing (for a given lift coefficient of 0.5 and a given thickness ratio of 14 %) the free-stream Mach number M_∞, and then maximizing at that Mach number (M_∞ = .7032) the minimum radius of curvature at the nose so that a nose as blunt as possible was obtained. In this way the parameters of profile E were found to be : M_∞ = .7032, Γ = .75, ε_o = .625, α = .055, M_c = .5193, θ_c = - 2.5094 degr., μ = .97.

The lifting quasi-elliptical profiles are practically symmetrical with nose camber only; they have a peaky pressure distribution. Though the peaky profiles have good transonic drag properties the question arises whether or not it would be better to try to design profiles with more blunt noses and with camber over the entire chord length in the hope to obtain profiles with for example better buffet boundaries.

In principle one may look for other profiles by using more parameters in the theory than the seven parameters already mentioned. It appears, however, that the appropriate choice of additional parameters presents severe numerical problems; encouraging results have not been obtained by us.

3 Experiments on a quasi-elliptical profile

General

A 180 mm chord model of quasi-elliptical profile E has been tested in the NLR transonic Pilot tunnel [9] in order to investigate the flow at and near the design condition and to determine the off-design behaviour, including the buffet boundary [10]. The Reynolds number based on chord length was about 2 million.

The design condition

When comparing the experimental with the theoretical results it was found useful to make a distinction between the theoretical and experimental design conditions. The reason for this is that the shock-free potential flow at the theoretical design condition (M_∞ = .7032, α = 2.6 degrees) is disturbed in the experiments by model imperfections, wind tunnel wall interference, the displacement effect of the boundary layer, and the fact that the Kutta-Joukowski condition will not be exactly satisfied at the tail of the profile because of the presence of a boundary layer. Due to these disturbing factors the flow cannot be made entirely shock free in the experiments. By varying the Mach number M_∞ and the model incidence α in a small range around the theoretical design values a flow condition was established for which the agreement between theory and experiment was best, using pressure measurements and optical observations as a guide. This condition was defined as the experimental design condition. It will be obvious that in this way corrections are made to the theoretical values of M_∞ and α for model imperfections, wall interference and boundary layer effects.

The theoretical and the experimental pressure distributions with natural transition and transition fixed are depicted in fig.7. In the experiments with transition fixed the roughness strips were postitioned between 9 and 10 % of the chord on the upper surface and between 17 and 18 % on the lower surface.

The agreement between theory and experiment is good. Very weak shocks are present at 40 % of the chord in the natural transition case and at 25 % in the fixed transition case (positions determined from optical observations). The shock waves are weakest with natural transition. In the natural transition case the pressure distribution is affected by a separation bubble on the upper surface between 18 and 25 % of the chord (determined with oil surface techniques). The discrepancies over the last 10 % of the chord are due to rapid boundary layer growth. From a pressure versus thickness plot (fig.8) it may be seen that there are small discrepancies between theory and experiment in expansion rate from the stagnation point up to the suction peak on the upper surface; these are mainly due to boundary layer growth and very small deviations of the model contour from the theoretical contour.

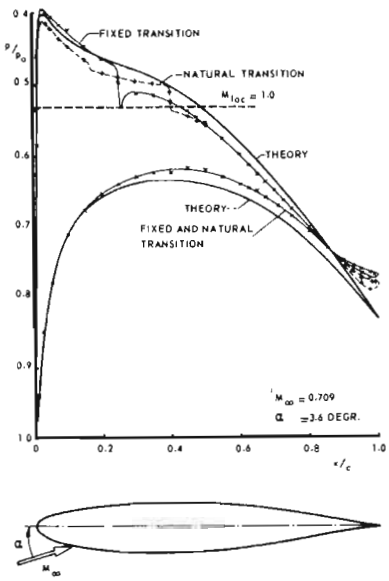

FIG. 7 PRESSURE DISTRIBUTIONS IN THE THEORETICAL AND EXPERIMENTAL DESIGN CONDITIONS. (PROFILE E)

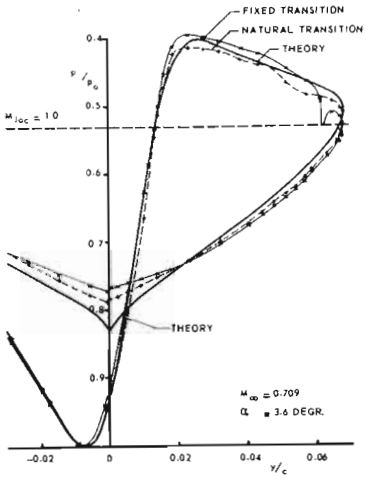

FIG. 8 PRESSURE DISTRIBUTIONS IN THE THEORETICAL AND EXPERIMENTAL DESIGN CONDITIONS.

These discrepencies should be kept as small as possible in the nose region because a large part of the flow in the supersonic region is determined by the expansion of the flow between stagnation point and suction peak.

Shadow photographs obtained with a continuous light source and with a short-duration spark exposure (1 μ sec) are given in fig.9. The first photograph shows a stationary short weak shock wave, the second one shows weak upstream moving disturbancies.

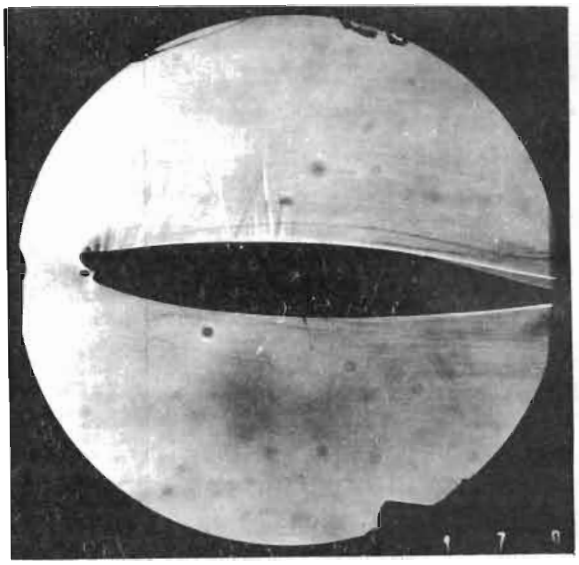

VISUALISATION OF STEADY FLOW (EXPOSURE TIME 1/250 SEC)

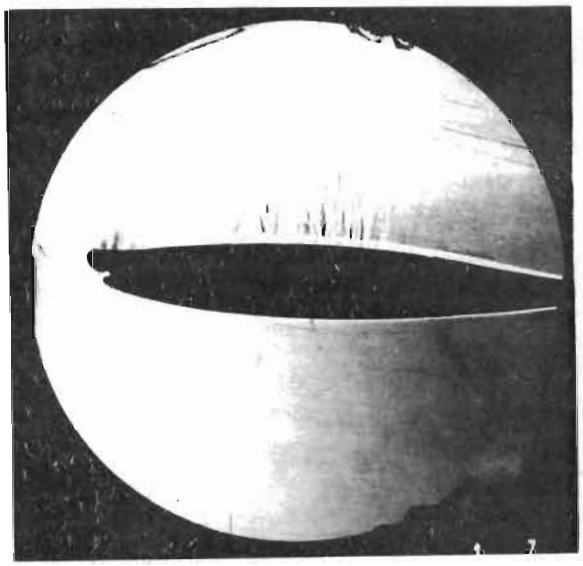

VISUALISATION OF WEAK UNSTEADY, UP STREAM MOVING DISTURBANCES (EXPOSURE TIME 10^{-5} SEC).

FIG. 9 SHADOW PHOTOGRAPHS OF FLOW IN THE EXPERIMENTAL DESIGN CONDITION (NATURAL TRANSITION).

Flow behaviour near the experimental design condition

The effect of variations of Mach number around the experimental design Mach number on the development of shock waves can be analyzed with pressure distribution curves over the first 60 % of the upper surface because the major flow changes occur in this region. In fig.10 curves of the ratio of the local static pressure to the total pressure are given at natural transition. It can be seen, that the shock wave (which location was determined by optical observations) fits smoothly into the other pressure distributions. The same conclusions follow from the pressure distributions measured with transition fixed (fig.11). The main difference between natural and fixed transition is, that the shock waves are somewhat stronger in the case of fixed transition; this is due to a slight disturbing effect of the roughness strip at the upper surface.

Drag characteristics, corresponding to the pressure distribution curves of fig.10 and 11 and obtained from wake-rake pressure measurements are presented in fig.12. From this figure it follows that the drag due to shock waves remains small up to a Mach number of 0.73 (0.02 in excess of the experimental design Mach number). The difference in drag level between natural and fixed transition is mainly due to a smaller laminar and a larger turbulent friction contribution to the total drag in the case of fixed transition. The decrease in drag in the natural transition case between M_∞ = .70 and M_∞ = .73 is due to a downstream movement of the transition point on the upper surface with increasing M_∞ ; this movement may be expected from the results of the pressure measurements reproduced in fig. 10.

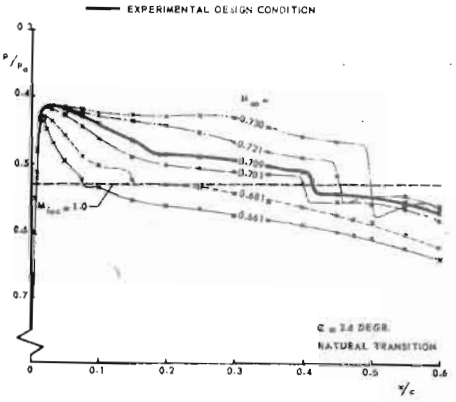

FIG. 10 EFFECT OF MACH NUMBER ON PRESSURE DISTRIBUTION NEAR EXPERIMENTAL DESIGN CONDITION.

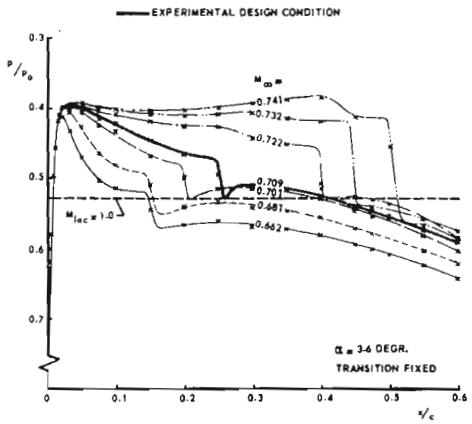

FIG. 11 EFFECT OF MACH NUMBER ON PRESSURE DISTRIBUTION NEAR EXPERIMENTAL DESIGN CONDITION.

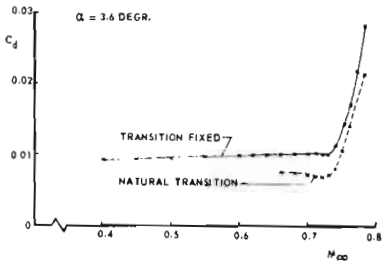

FIG 12 EFFECT OF MACH NUMBER ON DRAG COEFFICIENT AT EXPERIMENTAL DESIGN INCIDENCE.

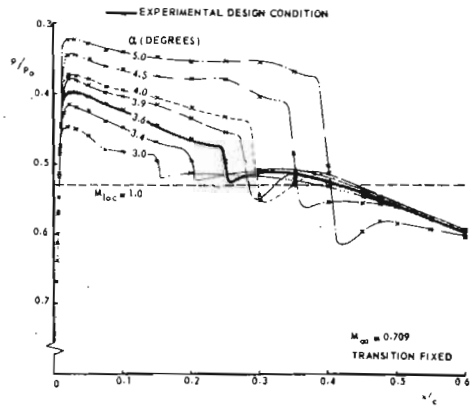

FIG. 13 EFFECT OF INCIDENCE ON PRESSURE DISTRIBUTION NEAR EXPERIMENTAL DESIGN CONDITION.

The effect of variations of the incidence around the experimental design incidence on the pressure distribution is given in fig.13 (fixed transition). The shook waves moves downstream and increases in strength with increasing incidence. The design condition fits smoothly into neighbouring flow conditions. From the corresponding drag coefficient-incidence plot (fig.14) it follows that the drag due to shock waves is small at incidences up to 4.0 degr.

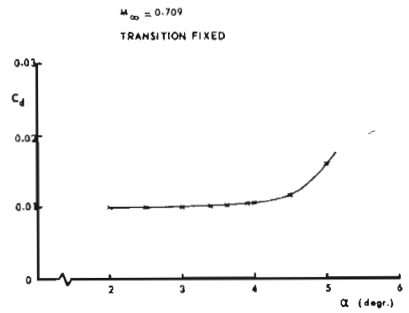

FIG. 14 EFFECT OF INCIDENCE ON DRAG COEFFICIENT AT EXPERIMENTAL DESIGN MACH NUMBER.

The existence of a margin around the experimental design condition where the drag due to shook waves is low can be correllated with two physical properties of the flow. The first is that the supersonic regions were observed to be low near the design condition; their heights are of the order of the model thickness. As a consequence, shock waves cannot extend far into the flow. The second is that near the design condition the shock waves remain weak due to the fact that a large part of the compression behind the suction peak is still built up by compressive waves originating at the sonic line as reflections of expansion waves generated at the model nose.

The effect of a trailing edge-flap deflection on lift and drag coefficients

It was already stated that discrepancies between theory and experiments may be expected due to the fact, that the Kutta-Joukowski condition is satisfied exactly in the theory, but not in the experiments because of the disturbing presence of the boundary layer at the tail. As a consequence the lift coefficient in the experimental design condition was about 20 % lower than the theoretical design value 0.5.

In order to be able to compensate this lift loss the model was provided with a trailing-edge flap with axis of rotation at 67.5 % of the chord. An experiment was performed with one degree flap deflection (δ = 1 degr.) and with transition fixed.

The effect of this flap deflection on the lift and drag coefficients as functions of the Mach number at the experimental design incidences is shown in fig. 15. It can be seen that the lift loss of about 20 % could be reduced to about 10 %. The drag rise Mach number decreased from 0.73 to 0.72. From the $c_p - M_\infty$ graph it follows that the effectiveness of the deflected flap decreases with increasing Mach number, which is due to an increase of the size of the supersonic region in the flow with increasing Mach number.

One can conolude, that a small deflection of a trailing edge flap (and hence introduction of a small amount of rear camber) increases the lift coefficients, but does not significantly impare the drag properties and thus the shock-free behaviour of the flow.

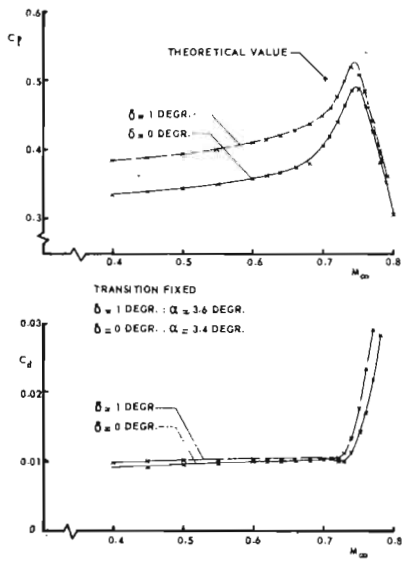

FIG. 15 EFFECT OF TRAILING-EDGE FLAP DEFLECTION ON LIFT AND DRAG COEFFICIENTS.

Buffet boundary

A buffet boundary was determined (δ = 0 degr., fixed transition) using rapid divergence of the trailing-edge pressure with incidence as a criterion for the onset of significant separation effects (fig.16). The rapid drag-rise boundary is also given. Furthermore a line is given showing where critical flow is reached. It can be seen that the margin between rapid drag-rise boundary and buffet boundary is rather small.

At Mach numbers below 0.7 approximately the buffet boundary lies at relatively low values of the lift coefficient. This is due to the fact that the model is nearly symmetrical (camber shifts the boundary to considerably higher values) and to the fact that the Reynolds number of the experiments was low (1 to 2.5 x 10^6, based on the model chord).

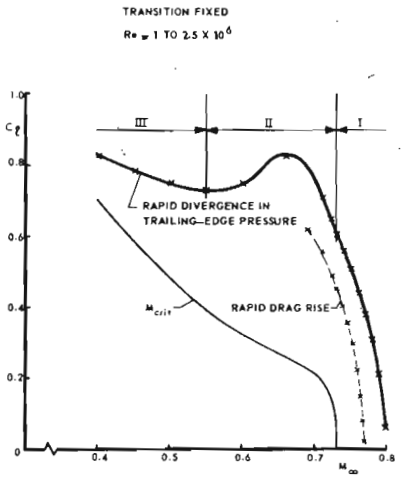

FIG. 16 RAPID DRAG-RISE AND TRAILING-EDGE PRESSURE DIVERGENCE BOUNDARIES.

When analyzing the onset of separation for increasing values of the incidence at a fixed Mach number, three regions may be distinguished in fig.16. In region I the onset of separation is characterized by a rearward development of a separation bubble at the foot of the shock wave. This type of separation is rather insensitive to Reynolds number variations provided the boundary layer is turbulent at the shock wave. The position of the buffet boundary in region II is determined by an interaction between a separation bubble at the foot of the shock wave and rear separation, in region III by rear separation combined with laminar separation bubbles just behind the suction peak.

Rear separation effects are Reynolds number dependent. It may be expected that at higher Reynolds number higher lift values will be found in regions II and III.

4 Conclusions

Profiles which have supercritical shock-free flow in the design condition can be computed with the quasi-elliptical profile theory. These profiles appear to be practically symmetrical with some nose camber only. The radius of curvature attains at the noses of the profiles smallest values of 1½ % of the chord or less. The pressure distribution in the design condition is of the peaky type. The height of the supersonic region is of the order of the profile thickness in the design condition.

The experiments have shown, that the theoretical design condition can be satisfactorily reproduced at an experimental design condition. The major difference is a 10 to 20 % loss in lift due to viscous effects at the tail of the profile. The shock waves are negligibly weak in the neighbourhood of the experimental design condition as the drag coefficient behaviour with Mach number and incidence shows. The lift losses can be compensated for at least partially by applying rear camber. The buffet boundary has at lower Mach numbers the characteristics of a symmetrical profile.

5 References

1. Nieuwland, G.Y. Transonic potential flow around a family of quasi-elliptical aerofoil sections. NLR-TR T.172, 1967.

2. Boerstoel, J.W. A survey of symmetrical transonic potential flows around quasi-elliptical aerofoil sections. NLR-TR T.136, 1967.

3. Baurdoux, H.I. and J.W. Boerstoel. Symmetrical transonic potential flows around quasi-elliptical aerofoil sections. NLR-TR 69007 U, 1969.

4. Spee, B.M. and R. Uijlenhoet. Experimental verification of shock-free transonic flow around quasi-elliptical aerofoil sections. NLR-MP 68003 U, 1968.

5. Nieuwland, G.Y. and B.M. Spee. Transonic shock-free flow, fact or fiction? NLR-MP 68004 U, 1968, (also in Proc. AGARD Spec. Meeting on Trans.Aarod., Sept. 68, Paris).

6. Spee, B.M. Investigations on the transonic flow around aerofoils. NLR TR 69122 U, 1969.

7. Van Eek, G.M. and J.W. Boerstoel. Qualitative results of the computation of transonic potential flows over lifting quasi-elliptical profiles. Internal NLR report AT-69-07, 1969 (classified).

8. Boerstoel, J.W., G.M. van Eek and G.H. Huizing. Results of the computation of the section data of sub- and super-critical lifting quasi-elliptical profiles. Internal NLR report AT-69-06, 1969 (classified).

9. Zwaaneveld, J. Principal data of the NLR Pilot tunnel. NLR report MP 185 (1959).

10. Uijlenhoet, R. and J.A. van Egmond. A two-dimensional wind tunnel investigation on the flow and force characteristics of a lifting quasi-elliptical aerofoil section designed for transonic shock-free flow, Internal report NLR TR 70015 C, 1970 (classified).